

## **INSTABILITY OF VISCOUS INCOMPRESSIBLE FLOW IN A CHANNEL WITH TRANSVERSELY CORRUGATED WALLS**

JACEK SZUMBARSKI

*Warsaw University of Technology, Institute of Aeronautics and Applied Mechanics, Poland  
e-mail: jasz@meil.pw.edu.pl*

Destabilization of the laminar flow in a channel with transversely wavy walls is investigated. The basic flow is determined by a semi-analytical method based on the concept of immersed boundaries. The stability equations are discretized by the spectrally accurate Chebyshev-tau method. It is demonstrated that the transversal wall waviness can be used in order to achieve destabilization of the laminar flow at low Reynolds numbers. Possible applications include the improvement of mixing and heat/mass transfer in various devices used in heat technology, biotechnology and medicine.

*Key words:* wavy channel, laminar flow, linear stability

### **1. Introduction**

The enhancement of mixing is of crucial importance for efficient operation of such devices as compact heat exchangers, cooling systems in microelectronics, small bioreactors, oxygenators, dialysators and similar. Flows inside such devices are usually characterized by low or – at most – moderate Reynolds numbers (say, of the order of hundreds), thus they tend to be laminar with poor transport properties. The obvious way to improve the mixing is flow turbulence, however it can be hard to achieve. In some situations – like flows of suspensions of shear-sensitive biological material or blood – turbulence may be even undesirable. Then, improvement of the mixing must be achieved by an appropriate flow modification of the flow kinematical structure in the laminar (or transitional) regime.

It seems that the most widely analyzed method for the enhancement of mixing of internal laminar flows is the application of various variants of unidirectional wall waviness (taken in a broad sense, i.e. including such configurations like ribs or grooves) oriented parallel to the main flow direction. Such

wall waviness is referred here as the longitudinal one. In particular, in wall waviness presented in Fig. 1 would be considered longitudinal if the direction of the main flow was parallel to the  $0x$  axis of the reference frame.

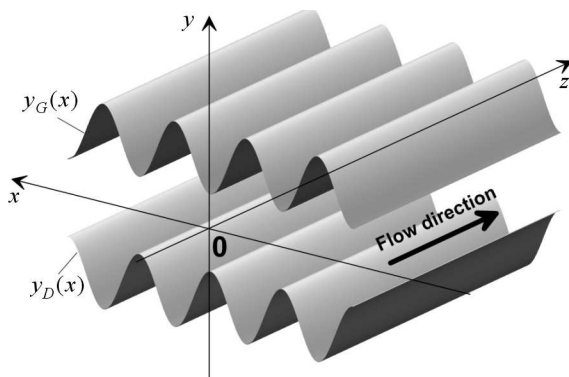


Fig. 1. A channel with sinusoidal wall waviness oriented transversely to the flow. The corrugation amplitude of both walls is the same while the phase is opposite. Thus, the flow domain is symmetric with respect to the plane  $y = 0$

During the last three decades, many variants of such geometrical modifications have been investigated both numerically and experimentally. First comprehensive experimental investigations of kinematical structures and mass transfer in the flow through a symmetric divergent-convergent channel with arc-shaped walls were carried out by Goldstein and Sparrow (1977). Numerical investigations of two-dimensional flow in a divergent-convergent symmetric channel (in two dimensions) with sinusoidal walls were performed by Sobey (1980) and verified experimentally by Stephanoff *et al.* (1980). Systematic investigations of flows in corrugated channels have been carried out since the middle 80s in Japan, mostly by Nishimura and his co-workers. They investigated a variety of kinematical structures, which appear in flows through channels with sinusoidal walls driven by steady (Nishimura *et al.*, 1990), pulsating (Nishimura *et al.*, 1989; Nishimura and Kawamura, 1995) and oscillatory pressure gradient (Nishimura *et al.*, 1987; Nishimura and Kojima, 1995). The basic conclusion from these works is that the significant improvement of mixing properties can be achieved when the natural flow separation phenomena cooperate with forced flow oscillations. Later, in numerical works by Ghaddar and El-Hajj (2000), Niceno and Nobile (2001), Wang and Vanka (1995) it was shown that a significant improvement of heat or mass transfer occurs only when the wall corrugation induces flow instability and the velocity field becomes oscillatory. For sinusoidal wavy walls with large amplitudes (reaching 27% of the average channel height), the oscillatory mode of the flow appears for the Reynolds number over 200 and more than threefold heat transfer enhancement (defined as the ratio between average Nusselt numbers for the flow

in the corrugated and plane channels) is achieved. A serious "penalty" for this improvement is the significantly increased hydraulic resistance, which can be even by order of magnitude larger than in the reference Poiseuille flow. This effect is especially severe when the corrugated walls have sharp edges (like in the case of the arc-shaped waviness).

Several authors have recently studied stability properties of laminar internal flows in the presence of a longitudinal wall corrugation. In the work by Cho *et al.* (1998), the linear stability of the laminar flow in the plane channel with sinusoidal walls is analyzed. Using a numerical solution to the linearized equations for small disturbances, the authors have shown the existence of two modes of instability: oscillatory and non-oscillatory. The first mode is attributed to traveling wave-like disturbances, and in fact it corresponds to the fundamental Tollmien-Schlichting (TS) wave modified by the presence of the wall waviness. The non-oscillatory mode corresponds to stationary (not traveling) disturbances. The critical Reynolds numbers (based on the average velocity and average half-distance between wavy walls) for both unstable modes depend of the corrugation amplitude and the spanwise wave number. For large corrugation amplitudes, two-dimensional TS waves are destabilized first, and the critical Reynolds number can drop to values as low as 100. The stationary disturbances are three-dimensional and for lower corrugation amplitudes their critical Reynolds number is smaller than for 2D TS waves. The effect of instability of TS waves on the effectiveness of heat transfer in the flow through a divergent-convergent channel was investigated numerically by Blancher *et al.* (1998). Recently, the same authors have carried out numerical analysis of spatially developing nonlinear instabilities in such a flow (Blancher *et al.*, 2004).

Some other works were originally motivated by the interest in the transitional phenomena in flows over rough walls rather than the mixing enhancement. For that reason, the amplitudes of the corrugation considered there are rather small and thus application of the perturbation methods is justified. Examples of such an approach can be found in Floryan *et al.* (2002), Selvarajan *et al.* (1999) or, recently, Wu and Luo (2006). Another possibility to investigate the stability of flows over slightly corrugated walls is to model the geometry modification by wall-distributed transpirations (blowing and suction). Using this approach, Floryan (1997) demonstrated that even small-amplitude, periodically distributed wall transpiration can significantly reduce the stability thresholds and that the unstable modes have a form of stationary streamwise-oriented vortices. Later, Szumbariski (2002c) showed that there exist two unstable modes and also the explained their origin. A computationally convenient setting for the investigation of a small or moderate wall corrugation is provided by the spectrally accurate method of immersed boundaries proposed originally in Szumbariski and Floryan (1999) and later extended by Szumbariski (2002b) to

linear stability equations. This method was successfully applied in the further works investigating the instability of the wavy-channel flows (Cabal *et al.*, 2002; Floryan, 2003, 2005; Szumbariski, 2002b) and, recently, also the phenomenon of transient growth of disturbances (Szumbariski and Floryan, 2006). The results of these works confirmed large potential of the small-amplitude wall waviness for flow destabilization. It has been established that wall corrugation with the amplitude equal only 2% of the average channel height can reduce the critical Reynolds number from 5772 (for the reference Poiseuille flow) to about 1000. They also allow one to properly interpret some results of the previous research. In particular to identify the 3-dimensional stationary modes discovered by Cho *et al.* (1998) as certain Squire modes modified by the presence of the wall waviness. High sensitivity of the critical conditions of the channel flow to small modifications such as a wall corrugation/transpiration or weak pulsations of the pressure gradient has been recently demonstrated by Wu and Luo (2006).

Surprisingly enough, the number of works investigating the stability of laminar flows in transversely corrugated channels is very limited. Such a type of geometrical modifications attracted some attention in the late 80's, mostly due to relations to surface elements known as "riblets". Most works on riblets are focused on the effect of reduction of the friction drag in turbulent boundary layers, see Viswanath (2002) for the recent review of the research in this field. Investigations of the laminar-turbulent transition in the boundary layer over riblet-mounted surfaces were carried in 90's, notably by Luchini (1995), Luchini and Trombetta (1995), Grek *et al.* (1996), Ehrenstein (1996). It has been established that the riblets affect the natural transition in the laminar boundary layer in the following manner: they accelerate the initial growth of the Tollmien-Schlichting waves but further nonlinear stage of transition (TS waves secondary instability, formation of lambda vortices and turbulent spots) is delayed and occurs farther downstream than in the case of a smooth surface. In the paper by Ehrenstein (1996) it was shown that the transversal short-period wall waviness destabilizes the originally two-dimensional Tollmien-Schlichting waves in the Poiseuille flow. For larger corrugation amplitudes, the critical Reynolds number of these disturbances can drop below 2600. This result is not very spectacular and actually seems to suggest that the transversal corrugation is by no means competitive to the longitudinal one as the method of the mixing enhancement. Indeed, similar reduction of the critical Reynolds number can be achieved with the use of the longitudinal waviness with the amplitude smaller by the order of magnitude and essentially without any noticeable increase in the flow resistance.

It is true indeed that the transversal waviness is much less efficient in destabilizing Tollmien-Schlichting waves than the longitudinal one. However, existence of some other forms of disturbances, which may be destabilized much

stronger than TS waves, cannot be excluded. We will show that such disturbances really exist and dramatic reduction of the critical Reynolds number of the flow can be achieved.

The paper is organized as follows. In Section 2, the problem of determination of the basic (undisturbed) flow is formulated and the semi-analytical method based on the concept of immersed boundaries is described. In Section 3, the linear stability of the basic flow is investigated. An unstable normal mode is identified and its parametric variation is studied numerically. Kinematic structures in the disturbance velocity field corresponding to the unstable mode are also presented. Finally, in Section 4, a short summary is provided and some conclusions are formulated.

## 2. Basic flow

### 2.1. Formulation of the problem

Let us first consider the reference case: laminar flow of a viscous liquid in a straight channel, i.e. in a region between two parallel flat walls. The coordinate system is chosen in such a way that the walls correspond to the planes  $Y = -H$  and  $Y = H$ . Let  $G_P < 0$  denote a constant pressure gradient which drives fluid motion in the positive direction of the  $Z$  axis. The velocity of the flow inside the channel takes the form

$$\mathbf{V}_0 = [0, 0, W_0(Y)] = \left[0, 0, W_{max} \left(1 - \frac{Y^2}{H^2}\right)\right] \quad (2.1)$$

where  $\mu$  denotes the dynamic viscosity and  $W_{max}$  is the maximum velocity given by the formula

$$W_{max} = -\frac{G_P H^2}{2\mu}$$

It is convenient to apply a dimensionless description. To this end, we define the length scale  $H$ , the velocity scale  $W_{max}$  and the pressure scale  $\rho W_{max}^2$ , where  $\rho$  denotes the density of the fluid. Then, velocity field (2.1) is transformed to the standard Poiseuille flow

$$w_0(y) = 1 - y^2 \quad (2.2)$$

where the dimensionless coordinate  $y$  belongs to the interval  $[-1, 1]$ . The non-dimensional pressure gradient can be now expressed by the Reynolds number  $\text{Re} = W_{max} H / \nu$  as

$$g_P = G_P \frac{H}{\rho W_{max}^2} = -\frac{2}{\text{Re}}$$

Let us consider now the laminar flow in the transversely wavy channel depicted in Fig. 1. In the dimensionless coordinates, the shape of the wavy walls is described by the following  $x$ -periodic functions

$$y_D(x) = -1 + S \cos(\alpha x) \quad y_G(x) = 1 - S \cos(\alpha x) \quad (2.3)$$

where  $S \geq 0$  is the amplitude of wall corrugation. Thus, the channel is symmetric with respect to the plane  $y = 0$ . The geometric period of the wall shape is  $\lambda_X = 2\pi/\alpha$ . The average height of the wavy channel is equal 2, i.e. it is the same as the wall distance in the reference straight channel.

The basic flow inside the wavy channel is assumed unidirectional and its velocity field can be expressed as

$$\mathbf{v}_B = [0, 0, W(x, y)] \quad (2.4)$$

Clearly, the continuity equation  $\operatorname{div} \mathbf{v}_B = 0$  is satisfied. We assume that the flow is driven by the same pressure gradient  $g_P$  as the reference Poiseuille flow.

The Navier-Stokes equation for the basic flow is reduced to the following Poisson equation

$$-g_P + \frac{1}{\operatorname{Re}} \Delta W = 0 \quad \Rightarrow \quad \Delta W = -2 \quad (2.5)$$

where  $\Delta = \partial_{xx} + \partial_{yy}$ . Since the function  $W$  is  $x$ -periodic, equation (2.5) should be satisfied in the domain  $\Omega = \{(x, y) : x \in (0, \lambda_X), y_D(x) < y < y_G(x)\}$ . The boundary conditions imposed at the channel walls are

$$W(x, y_D(x)) = 0 \quad W(x, y_G(x)) = 0 \quad (2.6)$$

## 2.2. Solution to the boundary value problem

In order to determine the basic flow, we take up a semi-analytical approach based on the concept of immersed boundaries. To this end, we define the extended computational domain  $\Omega_{ext} = \{(x, y) : x \in R, y \in [-1 - S, 1 + S]\}$ . Obviously, the inclusion  $\Omega \subset \Omega_{ext}$  holds.

Next, we assume that the basic flow is defined for every point in the extended domain  $\Omega_{ext}$ . The velocity of this flow can be written as the following sum

$$W(x, y) = w_0(y) + W'(x, y) \quad (2.7)$$

Expression (2.7) is admissible since formula (2.2) for the reference flow can be trivially extended to the interval  $[-1 - S, 1 + S]$ . The component  $W'(x, y)$  describes a modification of the reference flow due to the wall corrugation.

Equation (2.5) will be satisfied providing that the function  $W'(x, y)$  is  $x$ -periodic and harmonic, i.e. it fulfills the Laplace equation  $\Delta W' = 0$  in  $\Omega_{ext}$ .

The harmonic function  $W'$  can be expressed in the form of the Fourier series

$$W' = \sum_{n=-\infty}^{\infty} W_n(y)e^{in\alpha x} \qquad W_{-n} = W_n^* \qquad (2.8)$$

where the amplitude functions  $W_n$  are the solutions to the ordinary differential equations

$$(D^2 - n^2\alpha^2)W_n = 0 \qquad n = 0, \pm 1, \pm 2, \dots \qquad (2.9)$$

and can be expressed analytically as follows

$$W_0 = C_0 + S_0y \qquad (2.10)$$

$$W_n = C_n \cosh(n\alpha y) + S_n \sinh(n\alpha y)$$

Since the function  $W'$  is real, the coefficients  $C_0$  and  $S_0$  are real numbers and  $C_{-n} = C_n^*$ ,  $S_{-n} = -S_n^*$  for all  $n \neq 0$ . After insertion of (2.10) into (2.8), we get the formula

$$W'(x, y) = C_0 + S_0y + \sum_{n \neq 0} [C_n \cosh(n\alpha y) + S_n \sinh(n\alpha y)]e^{in\alpha x} \qquad (2.11)$$

The coefficients  $\{C_n\}$  and  $\{S_n\}$  should be such that the boundary conditions (2.6) are satisfied. Note that the wall contours  $y = y_D(x)$  and  $y = y_G(x)$  are "immersed" in the extended domain  $\Omega_{ext}$ , thus conditions (2.6) have internal rather than boundary character. The method used to enforce these conditions is similar to the immerse boundary technique described by Szumbariski and Floryan (1999). The basic idea is to calculate explicitly the Fourier coefficients of the velocity distributions at the wavy walls and then to make them vanish. Practically, only a certain number of the leading Fourier modes can be eliminated. In the current study, the least squares formulation of the elimination procedure is applied.

Consider the bottom wall of the channel  $y = y_D(x)$ . From (2.11), the velocity distribution at the bottom wall can be expressed as follows

$$\begin{aligned} W(x, y_D(x)) &= w_0(y_D(x)) + C_0 + S_0y_D(x) + \\ &+ \sum_{n \neq 0} [C_n \cosh(n\alpha y_D(x)) + S_n \sinh(n\alpha y_D(x))]e^{in\alpha x} \end{aligned} \qquad (2.12)$$

Since both the velocity field and the wall shape are periodic with respect to the  $x$  coordinate, the above formula describes the  $x$ -periodic function  $\varepsilon_D$ .

This function can be written in the form of the Fourier expansion

$$\varepsilon_D(x) \equiv W(x, y_D(x)) = \sum_{m=-\infty}^{\infty} E_m^D e^{im\alpha x} \tag{2.13}$$

We need to derive formulae for the coefficients  $\{E_m^D\}$ . To this end, the following Fourier expansions of all  $x$ -periodic functions appearing in equation (2.12) have to be calculated

$$\begin{aligned} w_0(y_D(x)) &= \sum_{m=-\infty}^{\infty} B_m^D e^{im\alpha x} \\ \zeta_m^D(x) \equiv \cosh(m\alpha y_D(x)) &= \sum_{n=-\infty}^{\infty} G_{m,n}^D e^{im\alpha x} \\ \gamma_m^D(x) \equiv \sinh(m\alpha y_D(x)) &= \sum_{n=-\infty}^{\infty} H_{m,n}^D e^{im\alpha x} \end{aligned} \tag{2.14}$$

Insertion of formulae (2.14) into (2.12) yields after some algebra the following expression for the function  $\varepsilon_D$

$$\varepsilon_D(x) = C_0 + \sum_{m=-\infty}^{\infty} \left( B_m^D + S_0 A_m^D + \sum_{n \neq 0} C_n G_{n,m-n}^D + \sum_{n \neq 0} S_n H_{n,m-n}^D \right) e^{im\alpha x} \tag{2.15}$$

Thus, for the bottom wavy wall we have

$$E_0^D = C_0 + B_0^D + S_0 A_0^D + \sum_{n \neq 0} C_n (G_{n,n}^D)^* + \sum_{n \neq 0} S_n (H_{n,n}^D)^* \tag{2.16}$$

$$E_m^D = B_m^D + S_0 A_m^D + \sum_{n \neq 0} C_n G_{n,m-n}^D + \sum_{n \neq 0} S_n H_{n,m-n}^D \quad m \neq 0$$

Analogous relations can be derived for the upper wall of the channel.

Boundary conditions (2.6) are enforced by setting

$$E_m^D = 0 \quad E_0^G = w_G \quad E_m^G = 0 \quad m = \pm 1, \pm 2, \dots \tag{2.17}$$

In practice, infinite Fourier expansions have to be truncated to a finite number of terms. Assume that, the summation in (2.8) is restricted to the Fourier modes with  $|n| \leq N$ , while conditions (2.17) are imposed for  $|m| \leq M$ . It is convenient to introduce  $4N + 2$  real unknowns: the real coefficients  $C_0$  and  $S_0$  and the real and imaginary parts of the remaining complex coefficients

$$\begin{aligned} C_m^R &= \mathcal{R}e(C_m) & C_m^I &= \mathcal{I}m(C_m) \\ S_m^R &= \mathcal{R}e(S_m) & S_m^I &= \mathcal{I}m(S_m) \end{aligned} \tag{2.18}$$

for  $n = 1, 2, \dots, N$ . After separation of the real and imaginary parts of equations (2.17) for  $m > 0$ , the following set of  $4M + 2$  linear algebraic equation is obtained ( $m = 1, 2, \dots, M$ )

$$\begin{aligned} & \frac{1}{2}C_0 + \frac{1}{2}A_0^{D,G}S_0 + \sum_{n=1}^N [\mathcal{R}e(G_{n,m}^{D,G})C_n^R + \mathcal{I}m(G_{n,m}^{D,G})C_n^I] + \\ & + \sum_{n=1}^N [\mathcal{R}e(H_{n,m}^{D,G})S_n^R + \mathcal{I}m(H_{n,m}^{D,G})S_n^I] = -\frac{1}{2}B_0^{D,G} \\ & \mathcal{R}e(A_m^{D,G})S_0 + \sum_{n=1}^N [\mathcal{R}e(G_{n,m+n}^{D,G} + G_{n,m-n}^{D,G})C_n^R + \mathcal{I}m(G_{n,m+n}^{D,G} - G_{n,m-n}^{D,G})C_n^I] + \\ & + \sum_{n=1}^N [\mathcal{R}e(H_{n,m+n}^{D,G} + H_{n,m-n}^{D,G})S_n^R + \mathcal{I}m(H_{n,m+n}^{D,G} - H_{n,m-n}^{D,G})S_n^I] = -\mathcal{R}e(B_m^{D,G}) \\ & \mathcal{I}m(A_m^{D,G})S_0 + \sum_{n=1}^N [\mathcal{I}m(G_{n,m+n}^{D,G} + G_{n,m-n}^{D,G})C_n^R - \mathcal{R}e(G_{n,m+n}^{D,G} - G_{n,m-n}^{D,G})C_n^I] + \\ & + \sum_{n=1}^N [\mathcal{I}m(H_{n,m+n}^{D,G} + H_{n,m-n}^{D,G})S_n^R - \mathcal{R}e(H_{n,m+n}^{D,G} - H_{n,m-n}^{D,G})S_n^I] = -\mathcal{I}m(B_m^{D,G}) \end{aligned} \tag{2.19}$$

where the upper indices  $D$  and  $G$  correspond to the bottom and upper wall, respectively. After system (2.19) is solved, the velocity field can be evaluated using formulae (2.7) and (2.11).

The properties of the above method were analyzed in details by Szumbarski (2007). It has been established that the method performs better when  $M > N$  and overdetermined linear system (2.19) is solved in the sense of the least squares (Golub and van Loan, 1996). If this system is written shortly as

$$\mathbf{P}\mathbf{c} = \mathbf{r} \tag{2.20}$$

where  $\mathbf{c} = [C_0, C_1^R, C_1^I, \dots, C_M^R, C_M^I, S_0, S_1^R, S_1^I, \dots, S_M^R, S_M^I]^T$ , then the least squares solution to (2.20) can be found by solving the following algebraic problem

$$\mathbf{P}^T\mathbf{P}\mathbf{c} = \mathbf{P}^T\mathbf{r} \tag{2.21}$$

with the symmetric and positive definite matrix  $\mathbf{Z} = \mathbf{P}^T\mathbf{P}$ . Linear system (2.21) can be solved by means of the  $QR$ -decomposition of the matrix  $\mathbf{P}$ , i.e.  $\mathbf{P} = \mathbf{Q}\mathbf{R}$ , where  $\mathbf{Q}$  denotes the orthogonal matrix (i.e.  $\mathbf{Q}^T\mathbf{Q} = \mathbf{I}$ ) and  $\mathbf{R}$  is the square upper-triangular matrix. Using the orthogonality of the matrix  $\mathbf{Q}$ , one gets from (2.21) the linear system

$$\mathbf{R}\mathbf{c} = \mathbf{Q}^T\mathbf{r} \tag{2.22}$$

which can be solved by the elementary back-substitution technique. The  $QR$ -decomposition of the matrix  $\mathbf{P}$  can be computed effectively by the modified Gram-Schmidt or Householder methods (Golub and van Loan, 1996).

### 2.3. Numerical tests

We will present some results of the numerical tests of the method described above. We will be mostly interested in the accuracy of the enforcement of boundary conditions (2.6). For symmetry reasons, the norm of the boundary error can be defined as follows

$$\varepsilon = \sup_{x \in [0, \lambda_X]} |W(x, y_D(x))| = \sup_{x \in [0, \lambda_X]} |W(x, y_G(x))| \quad (2.23)$$

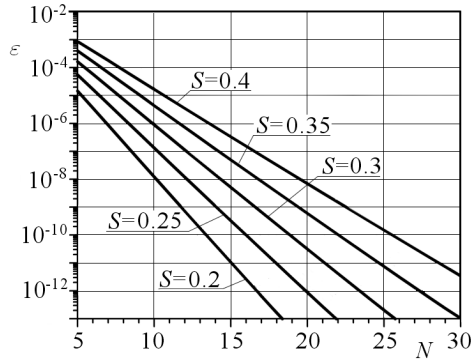


Fig. 2. The norm of the boundary error  $\varepsilon$  plotted versus the number  $N$  of Fourier modes used for approximation of the basic (undisturbed) flow, computed for different values of the amplitude  $S$ ; the wave number is  $\alpha = 1$

In all tests presented here it has been set  $M = 4N$ . In Fig. 2, the norm  $\varepsilon$  is plotted as a function of the number  $N$  of the Fourier modes, computed for different values of the corrugation amplitude  $S$  and the wave number  $\alpha = 1$ . It can be seen that the boundary error diminishes at an exponential rate, so the method is spectrally convergent. Obviously, the rate of convergence for larger corrugation amplitudes is slower. Figure 3 shows analogous results, but this time the amplitude  $S$  is fixed ( $S = 0.3$ ) and the parameter is the wave number  $\alpha$ . Again, the norm  $\varepsilon$  decreases asymptotically at the exponential rate, which, however, drops when the wave number  $\alpha$  increases.

The contour map of the velocity field of the basis flow computed for the amplitude  $S = 0.4$  and the wave number  $\alpha = 1$  is shown in Fig. 4. The maximum velocity (about 1.5) is achieved at the locations of the largest distance between walls, while its value at the narrowest part of the channel is about 3 times smaller. Thus, we observe strong spanwise modulation of the velocity, especially in the plane of symmetry  $y = 0$ .

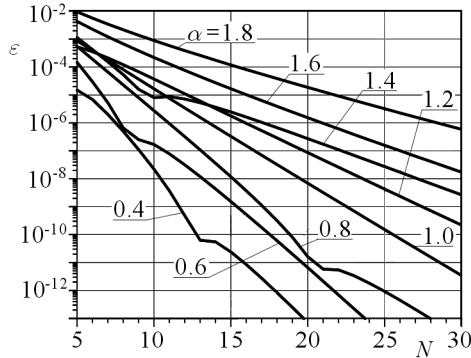


Fig. 3. The norm of the boundary error  $\varepsilon$  plotted versus the number  $N$  of Fourier modes used for approximation of the basic (undisturbed) flow, computed for different values of the amplitude number  $\alpha$ ; the corrugation amplitude is  $S = 0.3$

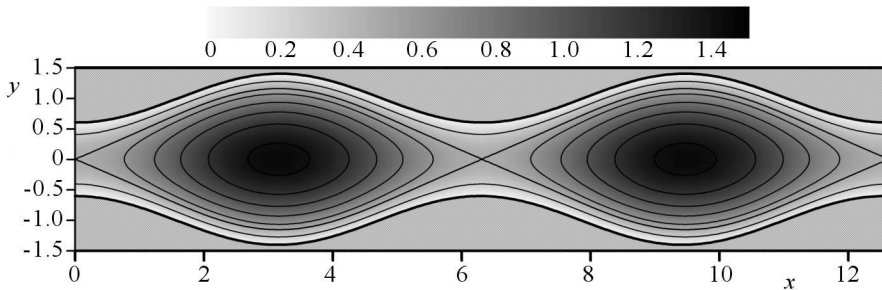


Fig. 4. A contour plot of the streamwise velocity of the basic flow in channel with symmetric transverse wall waviness. The amplitude is  $S = 0.4$  and the wave number is  $\alpha = 1$ . Note that the basic flow is unidirectional, i.e. the velocity components in the planes  $z = \text{const}$  vanish identically

It is important to evaluate the hydraulic resistance of the flow in the wavy channel. Note that the cross-sectional segments with the spanwise length equal to one geometric period  $\lambda_X$  taken from the wavy-wall and the reference channels have the same areas. In addition, the pressure drop driving both the reference and basic flow is the same. Thus, an appropriate way of evaluation of the flow resistance is to compare the volumetric flow rates computed per one geometric period. The results of such calculations, obtained for different values of  $S$  and  $\alpha$ , are presented in Fig. 5. The remarkable feature of the plotted lines is that they all intersect for  $\alpha \approx 1.2$ , where the ratio between the volumetric rates is very close to 1. It is also observed that the long-wave transversal corrugation leads to some reduction of the flow resistance, while for the shorter-wave corrugation the hydraulic losses increase with both  $\alpha$  and the amplitude  $S$ .

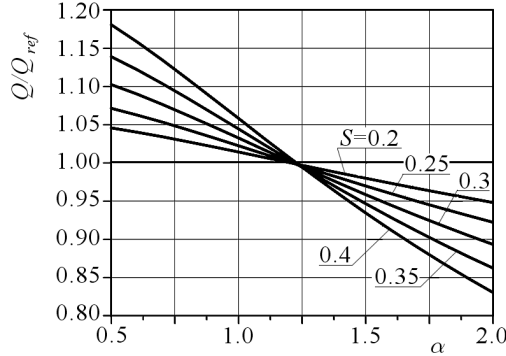


Fig. 5. The ratio between the volumetric flow rates in the wavy and plain channel flow plotted versus the wave number  $\alpha$  for different values of the corrugation amplitude  $S$

### 3. Analysis of linear stability

#### 3.1. Derivation of the stability equations

In this Section, we derive equations of the linear stability theory for the flow in the transversely wavy channel defined in Section 2.

The velocity of the basic flow described in the previous Section can be written as  $\mathbf{v}_B = W(x, y)\mathbf{e}_z$ , while the pressure  $p_B$  is a linear function of the  $z$  coordinate. We introduce time-dependent disturbances  $\mathbf{v}' = \mathbf{v}'(t, x, y, z)$  and  $p' = p'(t, x, y, z)$ , i.e. the velocity and pressure of the disturbed flow can be written as

$$\mathbf{v} = \mathbf{v}_B + \mathbf{v}' \quad p = p_B + p' \tag{3.1}$$

The mathematical description of the spatio-temporal evolution of flow disturbances can be obtained by inserting (3.1) to the Navier-Stokes and continuity equations. Since the flow disturbances are assumed small, the nonlinear term in the Navier-Stokes equation can be neglected. Eventually, the following equations are obtained

$$\begin{aligned} \partial_t u + W \partial_z u &= -\partial_x p' + \frac{1}{\text{Re}} \Delta u \\ \partial_t v + W \partial_z v &= -\partial_y p' + \frac{1}{\text{Re}} \Delta v \\ \partial_t w + W \partial_z w + u \partial_x W + v \partial_y W &= -\partial_z p' + \frac{1}{\text{Re}} \Delta w \\ \partial_x u + \partial_y v + \partial_z w &= 0 \end{aligned} \tag{3.2}$$

Equations (3.2) contain four unknown scalar fields: three Cartesian components of the disturbance velocity field and the field of pressure disturbances.

The coefficients of these equations depend on two space coordinates:  $x$  (periodically) and  $y$ . We will consider a special class of solutions to equations (3.2) known as the normal modes. These solutions are crucial for the determination of the asymptotic behavior of small disturbances in the flow. For the case considered in this study, the velocity and pressure fields of the normal modes are defined by the following expressions

$$\begin{aligned}
 [u, v, w](t, x, y, z) &= e^{i(\delta x + \beta z - \sigma t)} \sum_{m=-\infty}^{\infty} [g_u^m, g_v^m, g_w^m](y) e^{im\alpha x} + C.C. \\
 p'(t, x, y, z) &= e^{i(\delta x + \beta z - \sigma t)} \sum_{m=-\infty}^{\infty} q^m(y) e^{im\alpha x} + C.C.
 \end{aligned}
 \tag{3.3}$$

where the symbol  $C.C.$  stands for the complex conjugate terms.

In the above, the symbol  $\beta$  denotes the streamwise wave number,  $\delta$  is the Floquet parameter and the number  $\sigma = \sigma_R + i\sigma_I$  is the complex frequency of the normal mode. Thus, formulae (3.3) describe disturbances, which are periodic in the  $z$  variable with the period  $\lambda_Z = 2\pi/\beta$ . The type of dependence with respect to the  $x$  variable is related to the Floquet parameter, or – more precisely – to the value of the fractional part of the ratio  $\delta/\alpha$ . If this number is irrational, then the disturbed flow is quasi-periodic in the  $x$  direction. Otherwise, the disturbance field is  $x$ -periodic, however the period can be equal to some multiplicity of the geometric period  $\lambda_X = 2\pi/\alpha$ . In fact, it is sufficient to consider  $\delta$  from the range  $[0, \alpha/2]$ .

The time variation of the normal mode is determined by its complex frequency  $\sigma$ . If  $\sigma_I$  is negative, then the mode is attenuated or stable. If  $\sigma_I$  is positive, then the mode is amplified or unstable. In  $\sigma_I = 0$  we say that the mode is neutrally stable or critical. As a rule, all normal modes are stable if the Reynolds number is sufficiently small. In the linear stability analysis, we usually look for the smallest value of the Reynolds (denoted by  $Re_L$ ) for which at least one neutrally stable normal mode exists. If  $Re > Re_L$ , some disturbances will exponentially grow in time no matter how small they are initially. We say that for  $Re > Re_L$  the basic (or undisturbed) flow becomes unstable with respect to disturbances with an arbitrary small amplitude.

The real part of the complex frequency determines kinematic character of the disturbance field. If  $\sigma_R$  is different from zero, the disturbances have a form of the traveling wave (the speed of this wave in the streamwise direction is equal  $\sigma_R/\beta$ ). Such disturbances are also referred to as the oscillatory ones because at any fixed point in space one observes a time-periodic modulation of the disturbance amplitude (superimposed on the exponential decay or growth). If  $\sigma_R = 0$ , then time variation of the amplitude of disturbances at any space location is monotonic (nonoscillatory); such disturbances are sometimes called

stationary.

Substitution of expressions (3.3) into equations (3.2) leads to a countable set of ordinary differential equations for the amplitude functions  $g_u^m, g_v^m, g_w^m$  and  $q^m, (m = 0, \pm 1, \pm 2, \dots)$ . The mathematical description of the disturbance dynamics can be simplified in a similar manner as in the case of parallel flows (see Schmid and Henningson (2001) for more details) by eliminating the pressure disturbance field and introducing the  $y$ -component of vorticity with the formula

$$\eta = \sum_{m=-\infty}^{\infty} \theta^m(y) e^{i(t_m x + \beta z - \sigma t)} + C.C. \tag{3.4}$$

where

$$\theta^m = i(\beta g_u^m - t_m g_w^m) \quad m = 0, \pm 1, \pm 2, \dots \tag{3.5}$$

and  $t_m = \delta + m\alpha$ . Using relations (3.5) together with the formulae implied by the continuity equations

$$it_m g_u^m + \partial_y g_v^m + i\beta g_w^m = 0 \quad m = 0, \pm 1, \pm 2, \dots \tag{3.6}$$

one can express the amplitude functions of the velocity components  $u$  and  $w$  by the velocity component  $v$  and the vorticity components  $\eta$ , namely

$$g_u^m = i \frac{t_m \partial_y g_v^m - \beta \theta^m}{k_m^2} \quad g_w^m = i \frac{\beta \partial_y g_v^m + t_m \theta^m}{k_m^2} \tag{3.7}$$

In the above, we have introduced the real numbers  $k_m^2 = t_m^2 + \beta^2$ , which must be different from zero for all integer indices  $m$ . The latter condition is always satisfied if the streamwise wave number  $\beta \neq 0$ , which is assumed in this study. The special case  $\beta = 0$  (meaning that the disturbance field does not actually depend on the streamwise coordinate  $z$ ) requires a separate treatment and it will not be considered here.

After some rather laborious algebra, the following set of equations can be derived ( $m = 0, \pm 1, \pm 2, \dots$ )

$$\begin{aligned} & -i\sigma L^m g_v^m + S^m g_v^m + \\ & + \sum_{n>0} (H_V^{m,n} g_v^{m-n} + \widehat{H}_V^{m,n} g_v^{m+n} + H_\theta^{m,n} \theta^{m-n} + \widehat{H}_\theta^{m,n} \theta^{m+n}) = 0 \\ & -i\sigma \theta^m + Q^m \theta^m - it_m DF_W^0 g_v^m + \\ & + \sum_{n>0} (E_V^{m,n} g_v^{m-n} + \widehat{E}_V^{m,n} g_v^{m+n} + E_\theta^{m,n} \theta^{m-n} + \widehat{E}_\theta^{m,n} \theta^{m+n}) = 0 \end{aligned} \tag{3.8}$$

The operators appearing in the above equations are defined as follows

$$\begin{aligned}
 L^m &= \partial_{yy} - k_m^2 & Q^m &= i\beta F_W^0 - \frac{1}{\text{Re}} L^m \\
 S^m &= i\beta(F_W^0 L^m - D^2 F_W^0) - \frac{1}{\text{Re}}(L^m)^2 \\
 H_V^{m,n} &= i\beta \left[ \frac{\beta^2 + t_{m-n}t_{m+n}}{k_{m-n}^2} F_W^n \partial_{yy} - (D^2 + k_m^2) F_W^n + \frac{2n\alpha t_{m-n}}{k_{m-n}^2} D F_W^n \partial_y \right] \\
 \hat{H}_V^{m,n} &= i\beta \left[ \frac{\beta^2 + t_{m-n}t_{m+n}}{k_{m+n}^2} (F_W^n)^* \partial_{yy} - (D^2 + k_m^2) (F_W^n)^* + \right. \\
 &\quad \left. - \frac{2n\alpha t_{m+n}}{k_{m+n}^2} (D F_W^n)^* \partial_y \right] \\
 H_\theta^{m,n} &= -i \frac{2n\alpha\beta^2}{k_{m-n}^2} (F_W^n \partial_y + D F_W^n) \\
 \hat{H}_\theta^{m,n} &= i \frac{2n\alpha\beta^2}{k_{m+n}^2} [(F_W^n)^* \partial_y + (D F_W^n)^*] \\
 E_V^{m,n} &= i \frac{n\alpha}{k_{m-n}^2} (\beta^2 + t_m t_{m-n}) F_W^n \partial_y - i t_m D F_W^n \\
 \hat{E}_V^{m,n} &= -i \frac{n\alpha}{k_{m+n}^2} (\beta^2 + t_m t_{m+n}) (F_W^n)^* \partial_y - i t_m (D F_W^n)^* \\
 E_\theta^{m,n} &= i\beta \frac{\beta^2 + t_m t_{m-2n}}{k_{m-n}^2} F_W^n & \hat{E}_\theta^{m,n} &= i\beta \frac{\beta^2 + t_m t_{m+2n}}{k_{m+n}^2} (F_W^n)^*
 \end{aligned} \tag{3.9}$$

The question arises how to formulate appropriate boundary conditions for equations (3.8). Since the physical domain  $\Omega$  has been extended to the computational domain  $\Omega_{ext}$ , these equations are supposed to be satisfied in the interval  $-1 - S < y < 1 + S$ . However, the "classical" boundary conditions for the amplitude functions cannot be formulated. Instead, we have to derive some conditions for these functions which would be equivalent to the physical constraints imposed on the velocity disturbance field, namely

$$\begin{aligned}
 u(t, x, y_D(x), z) &= u(t, x, y_G(x), z) = 0 \\
 v(t, x, y_D(x), z) &= v(t, x, y_G(x), z) = 0 \\
 w(t, x, y_D(x), z) &= w(t, x, y_G(x), z) = 0
 \end{aligned} \tag{3.10}$$

Such conditions can be obtained by means of the immerse boundary approach developed by the author (Szumbarski, 2002a). The general idea is to derive explicitly formulae for the Fourier coefficients of the  $x$ -periodic distributions of the velocity components at both channel walls and then to demand that

these coefficients identically vanish. Such a formulation is actually equivalent to the following denumerable set of integral conditions

$$\sum_{m=-\infty}^{\infty} \int_0^{\lambda_X} [g_u^m, g_v^m, g_w^m](t, y_D(x)) e^{i(m-k)\alpha x} dx = 0 \tag{3.11}$$

$$\sum_{m=-\infty}^{\infty} \int_0^{\lambda_X} [g_u^m, g_v^m, g_w^m](t, y_G(x)) e^{i(m-k)\alpha x} dx = 0 \quad k = 0, \pm 1, \pm 2, \dots$$

With the use of relations (3.7), conditions (3.11) can be expressed in terms of the amplitude functions  $g_v^m$  and  $\theta^m$  ( $m = 0, \pm 1, \pm 2, \dots$ ).

**3.2. Spectral discretization of the stability equations and the boundary conditions**

In order to obtain a numerically tractable problem, we have to discretize differential equations (3.8) and to derive a finite dimensional approximation of integral conditions (3.11). To this end, we introduce truncated Chebyshev expansions

$$g_v^n(y) \approx \sum_{k=0}^{K_V} \Gamma_k^n T_k(y) \quad \theta^n(y) \approx \sum_{k=0}^{K_\theta} \Theta_k^n T_k(y) \tag{3.12}$$

where the basic functions are defined as  $T_k(y) = t_k[y/(1 + S)]$  and  $t_k$  denotes the "standard" Chebyshev polynomial of the  $k$ th order. For a detailed description of the properties of these polynomials, the reader may refer to Boyd (2001).

Next, finite Chebyshev expansions (3.12) are inserted into equations (3.8)<sub>1</sub>. Then each of these equations is multiplied by the polynomial  $T_j$  ( $j = 0, 1, \dots, K_V - 4$ ) and integrated in the interval  $[-1 - S, 1 + S]$  with the modified Chebyshev weight function

$$\omega(y) = \frac{1 + S}{\sqrt{(1 + S)^2 - y^2}} \tag{3.13}$$

Equivalently, it is demanded that the residua of all 4th order equations (3.8)<sub>1</sub> are  $\omega$ -orthogonal to the finite dimensional space of the polynomials of an order not higher than  $K_V - 4$ . As a result, a set of  $K_V - 3$  linear algebraic equations is obtained for each integer number  $m$ . Analogous procedure applied to the 2nd order differential equations (3.8)<sub>2</sub> produces  $K_\theta - 1$  algebraic equations for each integer index  $m$ . This way, the number of algebraic equations obtained due to the Chebyshev-Galerkin projection for the  $m$ th Fourier mode of the

disturbance field is equal to  $K_V + K_\theta - 4$ , while the number of unknowns corresponding to this mode is  $K_V + K_\theta + 2$ . Thus, for each integer  $m$  one is free to add six algebraic equations in order to enforce boundary constraints (3.11).

We will skip writing an explicit form of the algebraic equations obtained in effect of the discretization procedure because it has been described in details elsewhere (Szumbariski, 2002a, 2007). For practical calculations, the Fourier representation of the disturbance field has to be truncated to a finite number of modes. To this end, we will assume that all Fourier modes with the index  $m$  outside the range  $\{-M, \dots, M\}$  are omitted. This way we obtain  $(2M_S + 1)(K_V + K_\theta + 2)$  linear algebraic equations with the unknown Chebyshev coefficients  $\{\Gamma_k^m, k = 0, \dots, K_V, |m| \leq M_S\}$  and  $\{\Theta_k^m, k = 0, \dots, K_\theta, |m| \leq M_S\}$ . If we define the vector

$$\begin{aligned} \mathbf{z} &= \left[ \{\Gamma_0^n, \Gamma_1^n, \dots, \Gamma_{K_V-1}^n, \Gamma_{K_V}^n; \Theta_0^n, \Theta_1^n, \dots, \Theta_{K_\theta-1}^n, \Theta_{K_\theta}^n\}, n = \right. \\ &= \left. -M_S, \dots, 0, \dots, M_S \right]^T \end{aligned} \tag{3.14}$$

then the algebraic system can be conveniently written in a matrix-vector form as follows

$$\mathbf{Pz} = i\sigma\mathbf{Qz} \quad \mathbf{Bz} = \mathbf{0} \tag{3.15}$$

Thus, the normal modes are approximated by the eigenvectors of generalized eigenvalue problem (3.15) and the complex frequencies are simply the corresponding eigenvalues. In the current study, we are interested in flow destabilization, so we will look for the normal mode with the largest imaginary part  $\sigma_I$  and investigate its parametric variation.

### 3.3. Numerical analysis of an unstable normal mode

Investigation of unstable modes can be a tedious numerical task because of the number of parameters involved (wave numbers, Floquet parameter, amplitude of the wall corrugation and the Reynolds number) and the size of eigenvalue problem (3.15). The exact number of equations in (3.15) cannot be established *a priori* (the convergence analysis can be done only after an appropriate eigensolution has been identified), but on the basis of the author's previous experience a size of 2000-3000 can be anticipated. These expectation has been actually confirmed, and some results of the convergence study are presented in the Appendix.

The searching for unstable modes can be perform efficiently done by parametric continuation of the selected eigensolution of the Orr-Sommerfeld and Squire equations corresponding to the reference Poiseuille flow. A natural continuation parameter is the amplitude of the wave corrugation  $S$ . The numeri-

cal tools for such continuations are the methods of inverse or subspace iterations (Golub and van Loan, 1996; Saad, 1992). The key problem is to identify the eigenmodes of the Poiseuille flow, which are most sensitive to destabilization, while the corrugation amplitude increases. Some of these modes are already known: Ehrenstein (1996) showed that a short-wave transversal corrugation (with  $\alpha$  around 12) can destabilize the least attenuated, originally two-dimensional Orr-Sommerfeld mode (or the Tollmien-Schlichting wave) and the critical Reynolds number  $Re_L$  of the flow can be reduced to 2600, approximately. Here, however, we are looking for a possibility of effective flow destabilization at the Reynolds numbers which are much lower. It turns out that such a possibility appears in the range of parameters that has not apparently been investigated before. In addition, the normal mode being destabilized is quite different than the modes investigated in the previous works. This mode turns out to be the least attenuated Squire mode denoted here as  $Sq_1$ . Originally (i.e. in the Poiseuille flow), the wave vector of this mode can be written as  $\boldsymbol{\kappa} \equiv [\kappa_x, \kappa_y, \kappa_z] = [0, 0, \beta]$ . It can be shown that the corresponding velocity field has only a transversal component (here, the  $x$ -component), which is periodic in the streamwise direction  $z$ . Moreover, in the Poiseuille flow, the mode  $Sq_1$  is damped for all Reynolds numbers.

The situation becomes quite different when the transversal waviness is introduced. If the corrugation wave number  $\alpha$  assumes values in some range around 1.2 then the imaginary part of the complex frequency  $\sigma_I$  of the mode  $Sq_1$  grows quickly with the increasing amplitude  $S$ , and the mode becomes unstable even though the Reynolds number is rather low. The variations of the imaginary part of the complex frequency of the mode  $Sq_1$  with the streamwise wave number  $\beta$  computed for the wall waviness with the amplitude  $S = 0.3$  and different various wave numbers  $\alpha$  are shown in Fig. 6. The Reynolds number corresponding to these results is only 100. The destabilization effect is most pronounced for the waviness with the wave number around 1.2, i.e. for the corrugation period which is about 3 times larger than the average wall distance (or the channel height) and about 10 times larger than for the corrugation considered in Ehrenstein (1996). The obtained results demonstrate the possibility of radical reduction of the critical Reynolds number, even much below the value of 100. It is also very important that such a spectacular effect is achieved without introducing any additional hydraulic drag. In fact, the volumetric flow rate of the flow in a wavy channel is slightly larger than in the case of the reference Poiseuille flow. Since the driving pressure drop and the area of the cross-section in both cases are the same, we conclude that the most destabilizing wall waviness actually leads also to some reduction of the hydraulic resistance. This feature is quite opposite to what is observed in the case of the longitudinal waviness with a similar amplitude, where significant increase of the hydraulic resistance is inevitable.

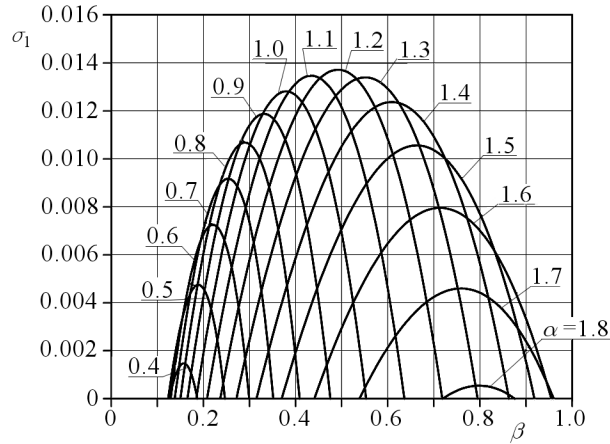


Fig. 6. The imaginary part of the complex frequency of the unstable normal mode  $Sq_1$  plotted versus the streamwise wave number  $\beta$ , computed for different values of the wave number  $\alpha$ . The amplitude of the wall waviness is  $S = 0.3$  and the Reynolds number is  $Re = 100$

The destabilization effect of the transversal waviness of the channel walls can be nicely illustrated by plotting the curve of neutral stability, i.e. the line in the  $Re$ - $\beta$  plane along which  $\sigma_I = 0$ . Such curves, calculated for three different values of the corrugation amplitude  $S$  and for the wave number  $\alpha = 1$ , are presented in Fig. 7. One can see that the critical Reynolds number  $Re_L$  for the amplitude  $S = 0.4$  is approximately equal to 58, hence it is smaller by two orders of magnitude (!) than  $Re_L$  for the reference Poiseuille flow.

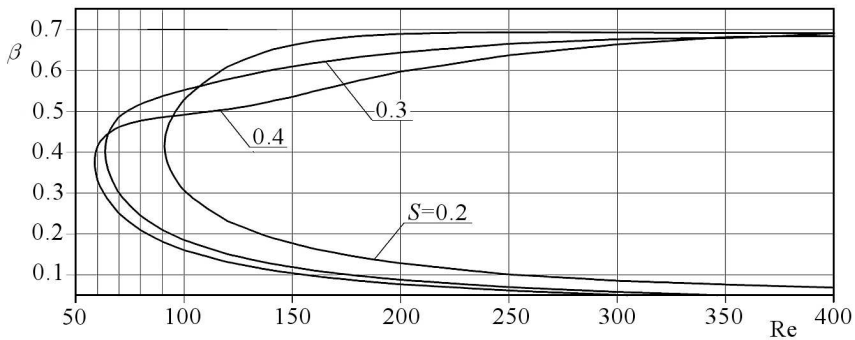


Fig. 7. Neutral stability curves of the mode  $Sq_1$  computed for different values of the corrugation amplitude  $S$ . The wave number  $\alpha = 1$

It is interesting to investigate the kinematical structure of the unstable mode  $Sq_1$  is presented in Fig. 8 and Fig. 9. The geometric parameters of the wall waviness are  $S = 0.4$  and  $\alpha = 1$ , the streamwise wave number  $\beta = 0.4$  and the Reynolds number is  $Re = 100$ . The disturbance velocity field has been nor-

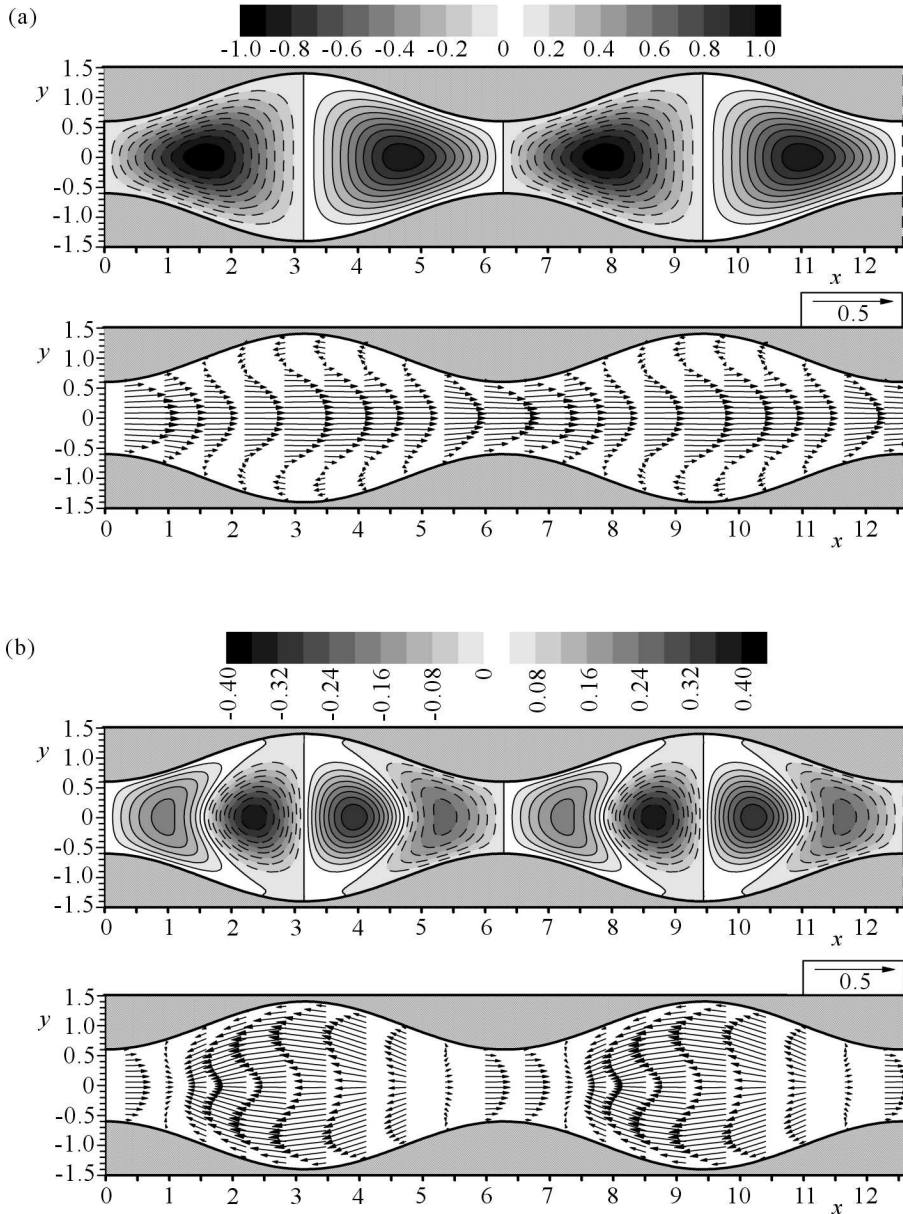


Fig. 8. The disturbance velocity fields of the unstable normal mode  $Sq_1$  computed at two channel sections: (a)  $z = 0$ , (b)  $z = \lambda_z/4$  for the Reynolds number is  $Re = 100$ , corrugation amplitude  $S = 0.4$  and wave number  $\alpha = 1$ . The streamwise wave number is  $\beta = 0.4$ . The contour maps show the streamwise velocity component  $w$  (dashed lines correspond to negative values). The velocity field is normalized so that its maximum magnitude in the flow domain is attained in the plane  $z = 0$  and equals 1

malized in such a way that the maximum of the velocity magnitude inside the channel is attained at the plane  $z = 0$  and is equal to 1. The spanwise structure of the velocity field at the plane  $z = 0$  is presented in Fig. 8a. The upper plot shows a contour map of the streamwise velocity component  $w$ , while the bottom one presents the velocity vectors projected on the plane of the section. Figure 8b shows analogous results computed for the plane  $z = \lambda_z/4 = \pi/2\beta$ . The structure of the velocity field in the symmetry plane  $y = 0$  is depicted in Fig. 9. The space-periodic system of counter-rotating vortices is clearly seen. All presented pictures give an idea of complicated three-dimensional kinematics of flow disturbances related to the unstable mode  $Sq_1$ . It should be emphasized that the real part of this mode is not zero, so the flow disturbances have a form of a traveling wave. The velocity of this wave in the streamwise direction is equal to the ratio  $\sigma_R/\beta$ , and in the case considered above, it is equal 0.854, which is close to the average velocity of the basic flow in the symmetry plane  $y = 0$ .

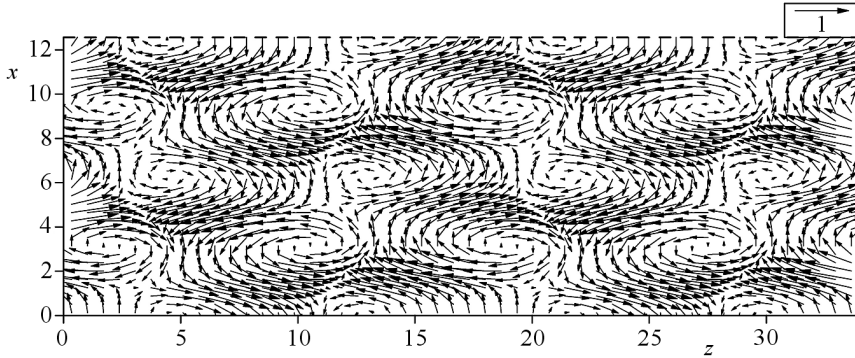


Fig. 9. The disturbance velocity fields of the instable mode  $Sq_1$  computed in the plane  $y = 0$  (the central plane of the wavy channel). All parameters and normalization are the same as in Fig. 8

#### 4. Summary and conclusions

In this study, the laminar viscous flow in a channel with transversely oriented wall waviness has been determined using a semi-analytical method of immersed boundaries which avoids the domain transformation. This method has been proved to be spectrally convergent, and if the geometric period of the wall waviness is large enough, it gives good accuracy even for relatively large corrugation amplitudes.

The linear stability analysis of the basic flow has been performed and the possibility of flow destabilization at the Reynolds number as low as 60 has been established. The wave number of the most destabilizing wall corrugations is about 1.2, which corresponds to the geometric period being about 3 times larger than the average channel height. The unstable normal mode originates from the fundamental Squire mode of the reference Poiseuille flow. Originally, this mode is attenuated and has a simple kinematical structure (its velocity has only a transversal component). The presence of wall waviness strongly destabilizes this mode, and the disturbance velocity field contains a system of counter-rotating vortices. The unstable disturbance field has a form of the wave which travels downstream with a velocity close to the average velocity of the undisturbed flow in the symmetry plane  $y = 0$  of the channel.

It can be expected that for the Reynolds numbers slightly higher than the critical value  $Re_L$ , the nonlinear saturation process of the unstable mode will occur. The new nonlinear state of flow, emerging due to the saturation process, would have a complex vortical structure, good mixing properties and hydraulic resistance comparable with the reference Poiseuille flow. One of possible ways to investigate the saturation process is to derive the low dimensional dynamical system out of the full Navier-Stokes equation using the Galerkin method and the normal modes of stability equations derived in the role of divergence-free basic functions. The obtained system of nonlinear ordinary differential equations can be solved numerically, and bifurcation behavior can be investigated. In further perspective, the properties of mass and heat transport of the saturated flow will also be investigated.

## Appendix

Here we present the results of convergence study for the spectral discretization method applied to the stability equations. The test calculations have been carried for the wave number  $\alpha = 1$ , the amplitude of the wall waviness  $S = 0.4$  and the Reynolds number  $Re = 100$ . For such parameters, the fundamental Squire mode  $Sq_1$  is unstable. In Table 1, we show the real and imaginary parts of the complex frequency  $\sigma$  of this mode as well as the value of the boundary error  $\varepsilon$ , i.e. the maximum magnitude of the disturbance velocity field at the channel walls. The velocity field of the mode has been normalized in such a way that the maximum velocity magnitude in the flow domain is 1. The number of Chebyshev polynomials used for approximation of the amplitude functions is  $K_V = K_\theta = 50$ .

Rapid convergence of the complex frequency is observed with the increasing number of the Fourier modes  $N$ . Note that high accuracy of  $\sigma$  is achieved in

spite of the relatively large boundary error. The latter decreases with  $N$  in the manner that proves spectral convergence of the approximation.

**Table 1**

$N$	$\sigma_R$	$\sigma_I \cdot 10^2$	$\varepsilon$
8	0.34174012	1.37161397	0.10651771
10	0.34171914	1.37262042	0.05299126
12	0.34171812	1.37276618	0.02218982
14	0.34171807	1.37277909	0.00994565
16	0.34171807	1.37278009	0.00471424

## References

1. BLANCHER S., CREFF R., LE QUERE P., 1998, Effect of Tollmien-Schlichting wave on convective heat transfer in a wavy channel. Part I: Linear analysis, *International Journal of Heat and Fluid Flow*, **19**, 39-48
2. BLANCHER S., CREFF R., LE QUERE P., 2004, Analysis of convective hydrodynamic instabilities in a symmetric wavy channel, *Physics of Fluids*, **16**, 10, 3726-3737
3. BOYD J.P., 2001, *Chebyshev and Fourier Spectral Methods*, 2nd Ed. Dover Publication Inc., Minneola NY
4. CABAL A., SZUMBARSKI J., FLORYAN J.M., 2002, Stability of flow in a wavy channel, *Journal of Fluid Mechanics*, **457**, 191-212
5. CHO K.J., KIM M., SHIN H.D., 1998, Linear stability of two-dimensional steady flow in wavy-walled channel, *Fluid Dynamic Research*, **23**, 349-370
6. EHRENSTEIN U., 1996, On the linear stability of channel flow over riblets, *Physics of Fluids*, **8**, 11, 3194-3196
7. FLORYAN J.M., SZUMBARSKI J., WU X., 2002, Stability of flow in a channel with vibrating walls, *Physics of Fluids*, **14**, 11, 3927-3936
8. FLORYAN J.M., 1997, Stability of wall-bounded shear layers in the presence of simulated distributed surface roughness, *J. Fluid Mech.*, **335**, 29-55
9. FLORYAN J.M., 2005, Two-dimensional instability of flow in a rough channel, *Physics of Fluids*, **17**, 044101-1 (electronic version)
10. FLORYAN J.M., 2003, Vortex instability in a diverging-converging channel, *J. Fluid. Mech.*, **482**, 17-50
11. GHADDAR N., EL-HAJJ A., 2000, Numerical study of heat transfer augmentation of viscous flow in corrugated channels, *Heat Transfer Engineering*, **21**, 35-46

12. GOLDSTEIN J.L., SPARROW E.M., 1977, Heat-mass transfer characteristics for flow in a corrugated wall channel, *Journal of Heat Transfer*, **99**, 187-195
13. GOLUB G.H., VAN LOAN CH.F., 1996, *Matrix Computations*, 3rd Ed., The John Hopkins University Press, Baltimore
14. GREK G.R., KOZLOV V.V., TITARENKO S.V., 1996, An experimental study of the influence of riblets on transition, *Journal of Fluid Mechanics*, **315**, 31-49
15. LUCHINI P., TROMBETTA G., 1995, Effects of riblets upon flow stability, *Applied Scientific Research*, **54**, 4, 313-321
16. LUCHINI P., 1995, Asymptotic analysis of laminar boundary-layer flow over finely grooved surfaces, *European Journal of Mechanics B Fluids*, **14**, 2, 169-195
17. NICENO B., NOBILE E., 2001, Numerical analysis of fluid flow and heat transfer in periodic wavy channel, *International Journal of Heat and Fluid Flow*, **22**, 156-167
18. NISHIMURA T., MURAKAMI S., ARAKAWA S., KAWAMURA Y., 1990, Flow observations and mass transfer characteristics in symmetrical wavy-walled channels at moderate Reynolds number for steady flow, *Int. J. Heat and Mass Transfer*, **33**, 835-844
19. NISHIMURA T., ARAKAWA S., MURAKAMI S., KAWAMURA Y., 1989, Oscillatory viscous flow in symmetric wavy-wall channels, *Chemical Engineering Science*, **44**, 2211-2224
20. NISHIMURA T., KAWAMURA Y., 1995, Three-dimensionality of oscillatory flow in a two-dimensional symmetric sinusoidal wavy-walled channel, *Exp. Therm. Fluid Sci.*, **10**, 62-73
21. NISHIMURA T., YOSHINO T., KAWAMURA Y., 1987, Numerical flow analysis of pulsatile flow in a channel with symmetric wavy walls at moderate Reynolds numbers, *J. Chem. Eng. Jpn.*, **20**, 479-485
22. NISHIMURA T., KOJIMA N., 1995, Mass transfer enhancement in a sinusoidal wavy-walled channel for pulsatile flow, *Int. Journal of Heat and Mass Transfer*, **38**, 1719-1731
23. SAAD Y., 1992, *Numerical methods for large eigenvalue problems*, Manchester University Press
24. SCHMID P.J., HENNINGSON D.S., 2001, Stability and transition in shear flows, *Applied Mathematical Sciences*, **142**, Springer, New York
25. SELVARAJAN S., TULAPURKARA E.G., VASANTA RAM V., 1999, Stability characteristics of wavy channel flows, *Physics of Fluids*, **11**, 3, 579-589
26. SOBEY I.J., 1980, On flow through furrowed channels. Part 1: Calculated flow patterns, *Journal of Fluid Mechanics*, **96**, 1-26
27. STEPHANOFF K.D., SOBEY I.J., BELLHOUSE B.J., 1980, On flow through furrowed channels. Part 2: Observed flow patterns, *Journal of Fluid Mechanics*, **96**, 27-32

28. SZUMBARSKI J., FLORYAN J.M., 1999, A direct spectral method for determination of flows over corrugated boundaries, *Journal of Computational Physics*, **156**, 378-402
29. SZUMBARSKI J., 2002c, On the origin of unstable modes in viscous channel flow subject to periodically distributed surface suction, *Journal of Theoretical and Applied Mechanics*, **40**, 4, 847-871
30. SZUMBARSKI J., 2002a, Immersed boundary approach to stability equations for a spatially periodic viscous flow, *Archives of Mechanics*, **54**, 3, 199-222
31. SZUMBARSKI J., 2002b, Linear Analysis of the disturbance dynamics in spatially periodic channel flow. Poster presentation [in Polish], *XV Polish Conference of Fluid Mechanics*, Augustów 2002
32. SZUMBARSKI J., FLORYAN J.M., 2006, Transient disturbance growth in a corrugated channel, *Journal of Fluid Mechanics*, **568**, 243-272
33. SZUMBARSKI J., 2007, Instability of the viscous liquid flow in the wavy-wall channel [in Polish], Habilitation Dissertation, In: *Prace Naukowe Politechniki Warszawskiej, Mechanika*, Warszawa
34. VISWANATH P.R., 2002, Aircraft viscous drag reduction using riblets, *Progress in Aerospace Sciences*, **38**, 571-600
35. WANG G., VANKA S.P., 1995, Convective heat transfer in periodic wavy passages, *Int. Journal of Heat and Mass Transfer*, **38**, 17, 3219-3230
36. WU X., LUO J., 2006, Influence of small imperfections on the stability of plane Poiseuille flow and the limitation of Squire's theorem, *Physics of Fluids*, **18**, 044104 (electronic form)

### Zjawisko destabilizacji przepływu laminarnego w kanale z poprzecznie pofalowanymi ścianami

#### Streszczenie

Praca poświęcona jest zjawisku destabilizacji przepływu laminarnego w kanale wywołanej poprzecznym pofalowaniem ścian. Przepływ niezaburzony wyznaczono przy pomocy semi-analitycznej metody zanurzonych granic. Wyprowadzono równania stateczności, które następnie poddano dyskretyzacji przy użyciu wielomianów Czebyszewa. Pokazano, że poprzeczne pofalowanie ścian o odpowiedniej geometrii prowadzi do destabilizacji przepływu przy niskich liczbach Reynoldsa i omówiono własności pola zaburzeń. Wydaje się, że opisany efekt może mieć znaczenie dla intensyfikacji mieszania i poprawy efektywności procesów transportu w technice cieplnej, biotechnologii i medycynie.